Biochimica et Biophysica Acta 1837 (2014) 899–907

Contents lists available at ScienceDirect

Biochimica et Biophysica Acta

journal homepage: www.elsevier.com/locate/bbabio

Disentangling two non-photochemical quenching processes in *Cyclotella meneghiniana* by spectrally-resolved picosecond fluorescence at 77 K

Volha U. Chukhutsina [a,b], Claudia Büchel [c], Herbert van Amerongen [a,b,d,*]

[a] Laboratory of Biophysics, Wageningen University, 6703HA Wageningen, The Netherlands
[b] BioSolar Cells, P.O. Box 98, 6700 AB Wageningen, The Netherlands
[c] Institute for Molecular Biosciences, Johann Wolfgang Goethe-University, 60438 Frankfurt am Main, Germany
[d] MicroSpectroscopy Centre, Wageningen University, 6703HA Wageningen, The Netherlands

ARTICLE INFO

Article history:
Received 13 January 2014
Received in revised form 17 February 2014
Accepted 19 February 2014
Available online 27 February 2014

Keywords:
Photosynthesis
Non-photochemical quenching
Diatom
Light-harvesting complex
Xanthophyll cycle

ABSTRACT

Diatoms, which are primary producers in the oceans, can rapidly switch on/off efficient photoprotection to respond to fast light-intensity changes in moving waters. The corresponding thermal dissipation of excess-absorbed-light energy can be observed as non-photochemical quenching (NPQ) of chlorophyll *a* fluorescence. Fluorescence-induction measurements on *Cyclotella meneghiniana* diatoms show two NPQ processes: qE_1 relaxes rapidly in the dark while qE_2 remains present upon switching to darkness and is related to the presence of the xanthophyll-cycle pigment diatoxanthin (Dtx). We performed picosecond fluorescence measurements on cells locked in different (quenching) states, revealing the following sequence of events during full development of NPQ. At first, trimers of light-harvesting complexes (fucoxanthin–chlorophyll *a*/*c* proteins), or FCPa, become quenched, while being part of photosystem II (PSII), due to the induced pH gradient across the thylakoid membrane. This is followed by (partial) detachment of FCPa from PSII after which quenching persists. The pH gradient also causes the formation of Dtx which leads to further quenching of isolated PSII cores and some aggregated FCPa. In subsequent darkness, the pH gradient disappears but Dtx remains present and quenching partly pertains. Only in the presence of some light the system completely recovers to the unquenched state.

1. Introduction

Diatoms are unicellular photosynthetic eukaryotes that are very abundant in water bodies and have a key role in the biochemical cycles of carbon, nitrogen, phosphorus and silica. They are thought to contribute ~20% to the global primary productivity, producing perhaps 20 Pg of carbon per year, and providing more oxygen than all tropical rainforests together [1,2]. Thriving in turbulent waters, diatoms have to cope with light-intensity fluctuations that can vary over several orders of magnitude on a timescale of seconds to minutes. In case of high-light stress the diatoms activate alternative energy sinks and dissipate excessively absorbed light through non-photochemical quenching (NPQ) in order to maintain an optimal photosynthetic activity.

Most of the photosynthesis processes take place in and around the thylakoid membranes, which in contrast to those of higher plants, are not segregated into stromal and granal regions. However, like in plants, their antenna complexes, the so-called fucoxanthin–chlorophyll *a*/*c* proteins (FCPs), are membrane-intrinsic (for reviews, see [1,3]). Although these antenna complexes belong to the light-harvesting chlorophyll (Chl) protein (LHC) superfamily [4], their pigment content differs considerably from that of light-harvesting complex (LHC) II in higher plants. FCPs do not possess Chl *b* but use Chl *c* as an accessory pigment, and they contain fucoxanthin (fx) as the major light-harvesting xanthophyll, which is not present in plants. Several studies have shown that red-absorbing fx forms (fx_{red}) are predominantly connected to PSII (photosystem II), whereas PSI receives relatively more excitation energy from the more blue-absorbing fx forms (fx_{blue}) [5,6]. The Chl *a* to carotenoid ratio is ~1 for diatom antenna complexes [7,8], whereas this number is ~3 for plants (see e.g. [9]). Two different major FCP complexes can be isolated from *Cyclotella meneghiniana*, the organism under investigation in the present study: trimeric FCPa and oligomeric FCPb that have similar spectroscopic properties but consist

Abbreviations: Chl, chlorophyll; DAS, decay-associated spectrum/spectra; Ddx, diadinoxanthin; Dtx, diatoxanthin; EET, excitation energy transfer; F_o, F_m, fluorescence yield measured with all reaction centers open (F_o) or closed (F_m); F_v/F_m, ratio of variable fluorescence to maximal fluorescence of dark-adapted sample with variable fluorescence being defined as $F_m - F_o$; F'_m, maximum fluorescence yield measured in the presence of high light with all reaction centers closed; F_t, initial (minimal) level of fluorescence in the presence of high light; FCP, fucoxanthin–chlorophyll $a/c_{1,2}$ protein; FCPa, trimeric fucoxanthin–chlorophyll protein complex a; FCPb, oligomeric fucoxanthin–chlorophyll protein complex b; fx, fucoxanthin; fx_{blue}, blue-absorbing fucoxanthin; fx_{red}, red-absorbing fucoxanthin; FWHM, full-width at half-maximum; LHC, light-harvesting chlorophyll protein; NPQ, non-photochemical quenching; OD, optical density; PS, photosystem; RC, reaction center; TCSPC, time-correlated single photon counting; qE, energy-dependent quenching; qI, photoinhibitory quenching; qT, state-transition quenching; XC, xanthophyll cycle

* Corresponding author at: Laboratory of Biophysics, Wageningen University, 6703HA Wageningen, The Netherlands. Fax: +31 317482725.
E-mail address: herbert.vanamerongen@wur.nl (H. van Amerongen).

http://dx.doi.org/10.1016/j.bbabio.2014.02.021
0005-2728/

of different polypeptides, with only FCPa complexes containing the light-harvesting complex stress-related protein subunits, denoted as Lhcx, needed for photoprotection [8,10–14].

In general, thermal energy dissipation via NPQ comprises a high-energy-state (qE), a state-transition (qT), and a photoinhibitory (qI) component (see e.g. [15]). In diatoms, NPQ is dominated by qE, whereas qT is missing [16] and qI is strongly reduced [17]. Diatoms have in common with vascular plants and green algae that the qE component is modulated by the conversion of xanthophyll cycle (XC) pigments. In diatoms, this comprises the de-epoxidation of diadinoxanthin (Ddx) to diatoxanthin (Dtx) (for a recent review see [18]). This conversion correlates with the build-up of NPQ, which is far more pronounced than in higher plants [19]. The quenching involves several components. One of them depends most probably directly on the light-driven proton gradient across the thylakoid membrane and it relaxes/disappears relatively fast upon switching to darkness [20] as can be observed by fluorescence induction measurements. Another one is thought to be directly related to the de-epoxidation of Ddx to Dtx [20,21].

In vitro, quenching of excitations can be induced via the aggregation of light-harvesting complexes, reducing excited-state lifetime and fluorescence yield [22], and this aggregation has often been implied to be responsible for NPQ in higher plants and algae, at least partly [23–26]. Based on picosecond spectroscopic studies NPQ in *C. meneghiniana* was also partly ascribed to aggregation of peripheral FCP complexes [27], whereas a second quenching process was postulated to be Dtx-dependent and to occur in an FCP complex close to the reaction center (RC) of PSII. It was suggested more recently [28] that the FCPa antenna might aggregate in *C. meneghiniana* upon lumen acidification, thereby leading to excited-state quenching. Furthermore, it was shown that the fluorescence yield of FCPa depends on the Dtx content in vitro, which is not the case for FCPb [29].

Although both fluorescence induction and picosecond spectroscopic measurements point at the presence of two different quenching mechanisms in *C. meneghiniana*, it has not been possible to correlate these to each other and to the in-vitro results on isolated (quenched and unquenched) antenna complexes. In the present study we prepare cells in different quenching states according to the fluorescence induction (PAM) measurements, stabilize these states by rapid cooling to 77 K and study the corresponding ultrafast kinetic and spectroscopic characteristics. By comparing our decomposed in vivo spectra with earlier reported in vitro spectra, a detailed model is proposed that reflects spectral and temporal characteristics of the various NPQ mechanisms in *C. meneghiniana* and pinpoints the locations where quenching takes place.

2. Materials and methods

2.1. Cell culture

The diatom *C. meneghiniana* (Culture Collection Göttingen, strain 1020-1a) was grown in batch cultures in Erlenmeyer flasks of 40 ml culture volume at 18 °C during constant shaking at 120 rpm at 20 μmol photons m^{-2} s^{-1} in the silica-enriched ASP medium according to [30]. A 16 h light:8 h dark cycle was used. Cells were harvested in the logarithmic growth phase. For all measurements 10 mM $KHCO_3$ was added to the algal cultures to ensure sufficient CO_2-supply during the periods of actinic high-light illumination.

2.2. Pigment preparation and analysis

Pigment stoichiometries of the cells were determined by analytical HPLC (Merck Elite LaChrom, L-2130/L-2450, Darmstadt, Germany). The cells were broken in 90% methanol buffered with 1 mM Tris pH 7.5 with 0.45 mm glass beads in a Bead Beater (BioSpec Products, Bartlesville, OK) for 9 min. Samples were centrifuged shortly at maximal speed in an Eppendorf centrifuge (Thermo Scientific, Langenselbold, Germany), and the supernatants were loaded onto the column. Pigments were separated and quantified using a RP18 column and a photodiode array detector as described previously [7].

2.3. PAM setup

Fluorescence induction kinetics of variable Chl fluorescence and the development of NPQ were monitored with a PAM fluorimeter (Walz GmbH, Effeltrich) on cells adjusted to a Chl *a* content of 2 μg ml^{-1} [31]. Saturating light flashes (3500 μmol photons m^{-2} s^{-1}) of 800 ms were applied every 2 min. The cells were dark adapted for 2 min before F_m was determined. Then the illumination protocol consisted of 10 min high-light illumination (~750 μmol photons m^{-2} s^{-1}), followed by 30 min of complete darkness ("relaxed" cells). The complete recovery of NPQ ("recovered" cells) was obtained when 30 min of low light (~10 μmol photons m^{-2} s^{-1}) followed 10 min of high-light illumination.

2.4. Measurements using the streak-camera setup

Time-resolved fluorescence experiments were performed at 77 K with a streak-camera setup [32–35], measuring fluorescence intensity as a function of wavelength and time. Three excitation wavelengths were used: 400 nm, 490 nm and 550 nm. The resulting images were corrected for background signal and detector sensitivity and sliced up into traces of 2 nm. The average of 100 images was taken, with each measured for 10 s. The laser power was in the range of 40–70 μW, the spot size was 100 μm, and the repetition rate was 250 kHz. Each sample was measured in 3 different states: original ("*unquenched*") state (taken directly from the growing chamber, followed by ~2 min of dark adaptation); "*quenched*" state (~10 min of white light preillumination at ~750 μmol photons m^{-2} s^{-1}); and "*relaxed*" (~30 min of darkness after 10 min of actinic light). Each measurement was repeated 3 times on different generations of the diatoms. Each generation was measured using two time windows: 800 ps and 2 ns.

The streak images were analyzed using the TIMP package for R language [36] and Glotaran, a graphical user interface for the R-package TIMP (glotaran.org). To get an equal good estimation of long (>700 ps) and short components, streak images obtained with different time windows were linked during the analysis. For the unquenched and relaxed states, datasets of different generations were linked. In the quenched situation, the datasets were analyzed independently, because of small variations in the amount of quenching between the measurements, but all trends and conclusions are fully consistent. A Gaussian-shaped instrument response function was used for the analysis and its width was a free fitting parameter. FWHM values obtained from the fitting procedure are in the range of 10–13 ps for the 800 ps time window and ~25–28 ps for the 2 ns time window. The synchroscan period (13.17 ns) results in a back and forth sweeping of long-lived components and leads to some signal "before time zero" in the streak-camera images [37]. This is used for the estimation of long lifetimes (many ns). The slowest component was always fixed to 3.7 ns. This lifetime was obtained independently for many datasets, but due to the limited time window of our setup, it was not possible to resolve it in a reliable way. The fit quality was judged by singular value decomposition of the residuals matrix (see also Supplemental Fig. 1) [36]. In the Supplemental Materials and methods it is described how the obtained DAS are decomposed into different components, like those of PSII and various antenna complexes.

3. Results and discussion

3.1. PAM measurements

First, we confirmed the presence of two different quenching processes using fluorescence induction measurements. Fluorescence and

NPQ induction of *C. meneghiniana* cells were recorded with the PAM setup and different quenched and unquenched states of the culture were characterized. The average F_v/F_m value for cells in growth conditions (before further measurements) was 0.60, which is close to values obtained previously for *C. meneghiniana*, grown in similar conditions ($F_v/F_m = 0.65$ [27], $F_v/F_m = 0.52$ [38]).

After determining F_v/F_m, high light of 760 μmol photons m^{-2} s^{-1} was applied for 10 min. Within a few seconds strong fluorescence quenching was observed (Fig. 1), which is believed to be partly triggered by a ΔpH across the photosynthetic membrane, that rapidly activates conversion of XC pigments [20]. The maximum fluorescence yield, measured in the presence of high light with all RCs closed (F_m') reached its highest amount of quenching during the first minute of illumination while the minimal fluorescence level in the presence of high light (F_t) continued to decrease during the whole illumination period and the dynamic control of this slower phase is achieved by the regulatory role of the XC carotenoids (*Ddx* and *Dtx*) [19–21,39]. Then the actinic light was switched off and cells were kept in complete darkness for 30 min. An immediate drop in NPQ was observed. This rapidly disappearing quenching is termed qE_1 (Fig. 1) and is thought to be directly linked to the drop in the pH gradient. Then both F_t and F_m' continued to increase but did not recover to the original level during these 30 mins. So around 5% of F_t remained quenched while for F_m' this was ~40%. It should be noted that NPQ remains present in complete darkness (qE_2) whereas it disappears in the presence of ~10 μmol photons m^{-2} s^{-1} (results not shown, see also [40]). qE_2 is supposedly regulated by Dtx [21,40], which is confirmed by pigment analysis (Table 1) of the cells measured in four different states: *unquenched*, *quenched*, *relaxed* (30 min in darkness) and *recovered* (in low light). *Relaxed* cells have almost identical Ddx and Dtx concentrations as *quenched* cells, confirming that indeed Dtx epoxidation is inhibited in complete darkness (see also [21]) whereas cells that recovered in low light have very similar amounts of Ddx and Dtx as cells in the unquenched state.

3.2. Picosecond kinetics of unquenched *C. meneghiniana* cells

In order to test the involvement of PSII and antenna complexes in NPQ, different pigment pools were selectively excited. Three excitation wavelengths were used: 550 nm light excites fx_{red} (antenna) preferably while 490 nm light excites both fx_{blue} and fx_{red} (antenna) [13,41]. At 400 nm mainly Chl *a* is excited [13,41] which is present in both photosystems as well as in FCPs [42].

Table 1
Pigment content of *C. meneghiniana* cells locked in four different states: unquenched, quenched, relaxed (in dark) and recovered (in low light). Pigment concentrations are presented as mM pigment M^{-1} Chl *a*. The table shows mean values with standard deviations of at least 3 measurements.

Sample	Pigment content (mM pigment M^{-1} Chl *a*)				
	Chl *c*	fx	Ddx	Dtx	β-Carotene
Unquenched	178 ± 10	692 ± 22	190 ± 18	28 ± 4	8 ± 2
Quenched	176 ± 4	658 ± 33	128 ± 12	82 ± 3	11 ± 5
Relaxed	172 ± 6	691 ± 17	123 ± 7	81 ± 5	11 ± 10
Recovered (in low light)	181 ± 16	686 ± 37	189 ± 20	30 ± 6	13 ± 7

Four decay components are sufficient to fit the fluorescence kinetics for all wavelengths. The resulting decay-associated spectra (DAS) for unquenched cells are shown in Fig. 2. The lifetimes are rather similar for all excitation wavelengths (Table 2). The total fluorescence spectra at t = 0 (sum of the corresponding DAS) were normalized to each other. They slightly differ in peak wavelength and amplitude for different λ_{ex} (Supplemental Fig. S2) and the corresponding DAS cannot be compared in absolute terms but their relative contributions can be judged. The shortest component has a DAS with positive peaks at 673 nm and 695 nm and negative peaks at 685 nm and 710 nm–720 nm. The corresponding excitation energy transfer (EET) from Chls with fluorescence peaking around 673 nm (Chl_{673}) to Chl_{685} is observed for all excitation wavelengths (positive/negative peaks at 673/685 nm) and is most pronounced for $\lambda_{ex} = 550$ nm, followed by $\lambda_{ex} = 490$ nm. Therefore, it largely represents EET within/between FCPs and from FCP towards PSII cores (see also [44], [45]), because more energy is transferred to PSII from fx_{red} than from fx_{blue} [5,6]. EET from $Chls_{695}$ to $Chls_{710–720}$ reflects excitation equilibration within PSI and the negative 710–720 nm peak corresponds to the 717 nm peak of PSI that is observed in steady-state fluorescence emission measurements at 77 K [43]. This process is most pronounced for 400 nm excitation.

The shape of the 2nd DAS (130–150 ps) indicates some EET from Chl_{682} to Chl_{692}. The area underneath the 680–682 nm band is higher for both fx excitation wavelengths, indicating that this corresponds largely to EET from FCP to PSII cores [5,6]. Apparently, there is heterogeneity in the transfer kinetics towards the core complexes, since the

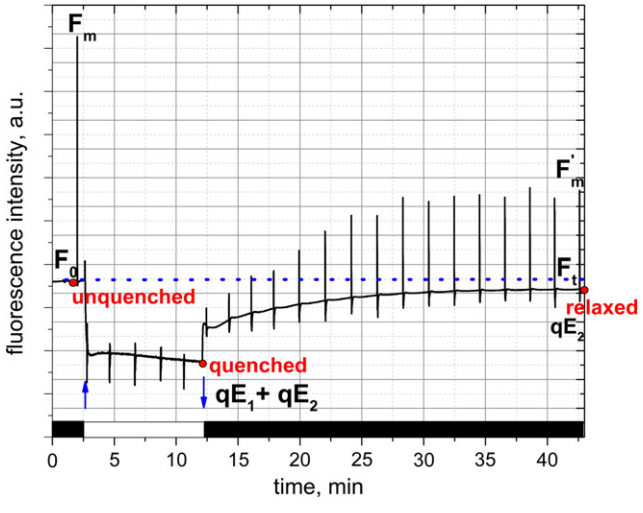

Fig. 1. Chl *a* fluorescence induction kinetics of *C. meneghiniana* cells. Samples were adjusted to 2 μg/ml. The figure depicts the transition from darkness to high light and to darkness again. High-light switch on/off is indicated by up/down arrows. The first saturating pulse was applied after 2 min of dark adaptation just before high light was switched on and the obtained F_v/F_m value is 0.60. *C. meneghiniana* was measured in complete darkness for 30 min after 10 min of high-light illumination. After 30 min of recovery in the dark, F_t and especially F_m' do not come back to the original level and stay quenched (original level of F_o is indicated by dotted line).

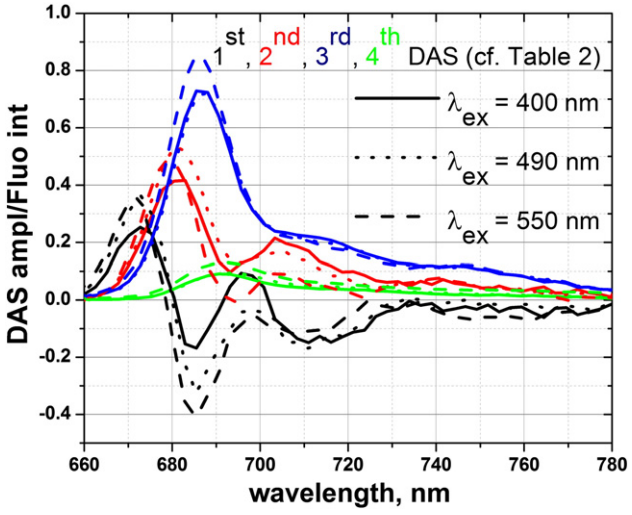

Fig. 2. DAS obtained from global analysis of streak-camera data measured at 77 K using unquenched cells for different excitation wavelengths: 400 nm (solid line), 490 nm (dotted line) and 550 nm (dashed line). For comparison, the total fluorescence spectra at t = 0 (which equals the sum of all DAS for a particular excitation wavelength) are normalized to their maximum (see Supplemental Fig. S2). The lifetimes of the corresponding DAS are presented in Table 2.

Table 2
Results of global fitting of the streak-camera data upon 400 nm, 490 nm and 550 nm excitation in unquenched, quenched and relaxed states.

Lifetimes, ps	λ_{ex}, nm	τ_1 (ps) black DAS	τ_2 (ps) red DAS	τ_3 (ps) blue DAS	τ_4 (ns) green DAS	τ_{avg} (ns) λ_{ex} = 685 nm	τ_{avg} (ns) λ_{ex} = 700 nm
Unquenched	400 nm	27	128	579	3.7	0.75	0.75
	490 nm	26	149	601	3.7	0.83	1.0
	550 nm	30	139	596	3.7	1.12	1.62
Quenched	400 nm	27	132	520	3.7	0.40	0.56
	490 nm	26	124	518	3.7	0.57	0.86
	550 nm	27	140	552	3.7	0.79	1.17
Relaxed	400 nm	25	128	580	3.7	0.63	0.75
	490 nm	28	145	600	3.7	0.83	1.02
	550 nm	30	143	604	3.7	1.12	1.62

Lifetimes estimated from global analysis of the fluorescence data obtained for the *C. meneghiniana* cells in different states. The DAS colors specified in the lifetimes rows correspond to the colors of the DAS in Figs. 2 and 4. Typical standard errors are 2.0–3.0% for τ_1, 0.5–1.0% for τ_2 and ~0.5% for τ_3 for all analyzed datasets. The slowest component is at the limit of the setup resolution and was always fixed to 3.7 ns. Average lifetimes of the total fluorescence decays were calculated at two detection wavelengths: 685 nm and 700 nm.

shape and amplitude of the 680–682 band differ for different fx excitation wavelengths. The "red" shoulder above 700 nm is largely due to PSI and its contribution decreases for excitation at longer wavelengths because fx_{blue} transfers more energy to PSI than fx_{red} [5,6] whereas fx_{red} excitation mainly leads to transfer to PSII [6]. The 3rd DAS component is to a large extent due to PSII. It peaks at ~685 nm which is close to the fluorescence emission bands of the PSII components at RT [6,27]. The 3.7 ns component has the smallest amplitude. The spectral shape with the peak near 690 nm and enhanced fluorescence above 720 nm very much resembles that of aggregated FCP antenna in vitro at 77 K [28].

It should be mentioned that no ns component with PSI characteristic was observed, in contrast to what was reported for native membranes of higher plants, where DAS with 2.3 ns and 7.4 ns lifetimes represent slow PSI trapping from red pigments [46]. It agrees however with previously reported steady-state 77 K measurements where the contribution of the PSI band is much smaller for diatoms than for plants [6,47].

In summary, in unquenched cells the fastest DAS reflects EET between the pigments of FCPs and into both photosystems, the second DAS is mainly due to EET into PSII together with charge separation in PSI, PSII dominates the 3rd DAS and the 4th DAS mainly reflects aggregated FCP complexes.

3.3. Picosecond kinetics of C. meneghiniana cells measured in different states

To discriminate between qE_1 and qE_2 *C. meneghiniana* cells were locked in three different states at 77 K: unquenched, quenched and relaxed. Typical streak-camera measurements are presented in Fig. 3 for the same 3 excitation wavelengths as used above. At all excitation wavelengths the fluorescence of unquenched cells (Fig. 3A, D, H) is longer-lived than for quenched cells (Fig. 3B, E, I) as expected, but when comparing unquenched and relaxed cells the situation is different. Upon exciting the outer antenna at either 490 or 550 nm the unquenched and relaxed cells show nearly identical kinetics, whereas λ_{ex} = 400 nm leads to clear differences. This immediately indicates that qE_2 is not related to the outer antenna FCP but must be related to PSII cores that are not or hardly connected to FCP.

3.3.1. Upon fx excitation only qE_1 is observed

First we analyzed streak-camera data measured upon fx excitation (490 and 550 nm) in different states to confirm that qE_2 is not monitored upon antenna excitation. So the resulting decay-associated spectra (DAS) for unquenched, quenched and relaxed cells are compared in Fig. 4A and B. Four components are sufficient to fit the data in all cases. Most lifetimes are similar for the different conditions except for τ_3 (blue DAS, Table 2), which is obviously shorter for quenched cells. However, the amplitudes of all four DAS differ substantially for the quenched and unquenched states, thereby strongly changing the average lifetime (Table 2) and fluorescence quantum yield (Supplemental Fig. S3). In agreement with Fig. 3, relaxed cells show nearly identical results as unquenched cells for 490 nm excitation and 550 nm excitation. The results for 490 nm excitation show a decrease in intensity upon quenching for the 3rd and 4th components leading to an increase of the shorter-lived 2nd component that peaks around 685 nm. The decrease of the 3rd DAS and the corresponding increase of the 2nd one are even larger for λ_{ex} = 550 nm excitation. The effect of qE_1 on the longest component is more or less the same for both fx excitation wavelengths and leads to a decrease of fluorescence peaking at around 690 nm. Summarizing, upon exciting the outer antenna complexes no effect of qE_2 is observed whereas qE_1 leads to a decrease of the relative amplitudes in the long-lived 3rd and 4th DAS and an amplitude increase of the short-lived 2nd DAS, thereby decreasing the total fluorescence quantum yield. The effect is largest upon 550 nm excitation where more PSII antenna is excited than at 490 nm [6].

3.3.2. Monitoring qE_1 and qE_2 upon Chl a (400 nm) excitation

The DAS for unquenched, quenched and relaxed cells upon 400 nm excitation are depicted in Fig. 4C. Most notably, the DAS of relaxed cells substantially differ from those of unquenched cells due to the effect of qE_2. Since this is not observed upon fx excitation (Fig. 3) it is concluded that PSII (core) complexes that are largely disconnected from FCPs are responsible for it. Upon going from the unquenched to the quenched states there is a strong decrease in the amplitude of the 3rd DAS whereas the corresponding lifetime is reduced by 60 ps (Table 2), which is also seen for fx excitation but to a lesser extent upon fx_{red} (550 nm) excitation. In darkness after high light illumination the amplitude of this component does not recover completely due to the remaining qE_2. Also the longest component is influenced by both qE_1 and qE_2 since its contribution drops by 55% upon quenching and its area recovers in complete darkness to only 85% of the original value. Upon quenching the main band of the 2nd component increases in intensity while the PSI shoulder hardly changes in amplitude. In darkness the amplitude of the main peak does not recover completely to the original state, demonstrating that not only qE_1 but also qE_2 leads to an increased contribution of the 2nd DAS. So upon exciting at 400 nm qE_1 is again observed but in addition qE_2 is now present which apparently occurs in PSII cores with little or no outer antenna connected. Because also Dtx remains present in the dark we conclude that it is involved in the quenching of these cores.

3.4. Spectral reconstruction upon antenna excitation describes qE_1

3.4.1. Evidence for PSII quenching

In order to attribute the different effects described above to certain photosynthetic protein complexes, we reconstructed spectra of separate emitting Chl *a* species from the obtained DAS, starting with that of PSII. The DAS with a clear PSII contribution is the 3rd component and upon quenching it shows a substantial decrease in amplitude for all excitation wavelengths. After subtracting the quenched 3rd DAS from the unquenched one (Fig. 5), we obtain a spectrum with the

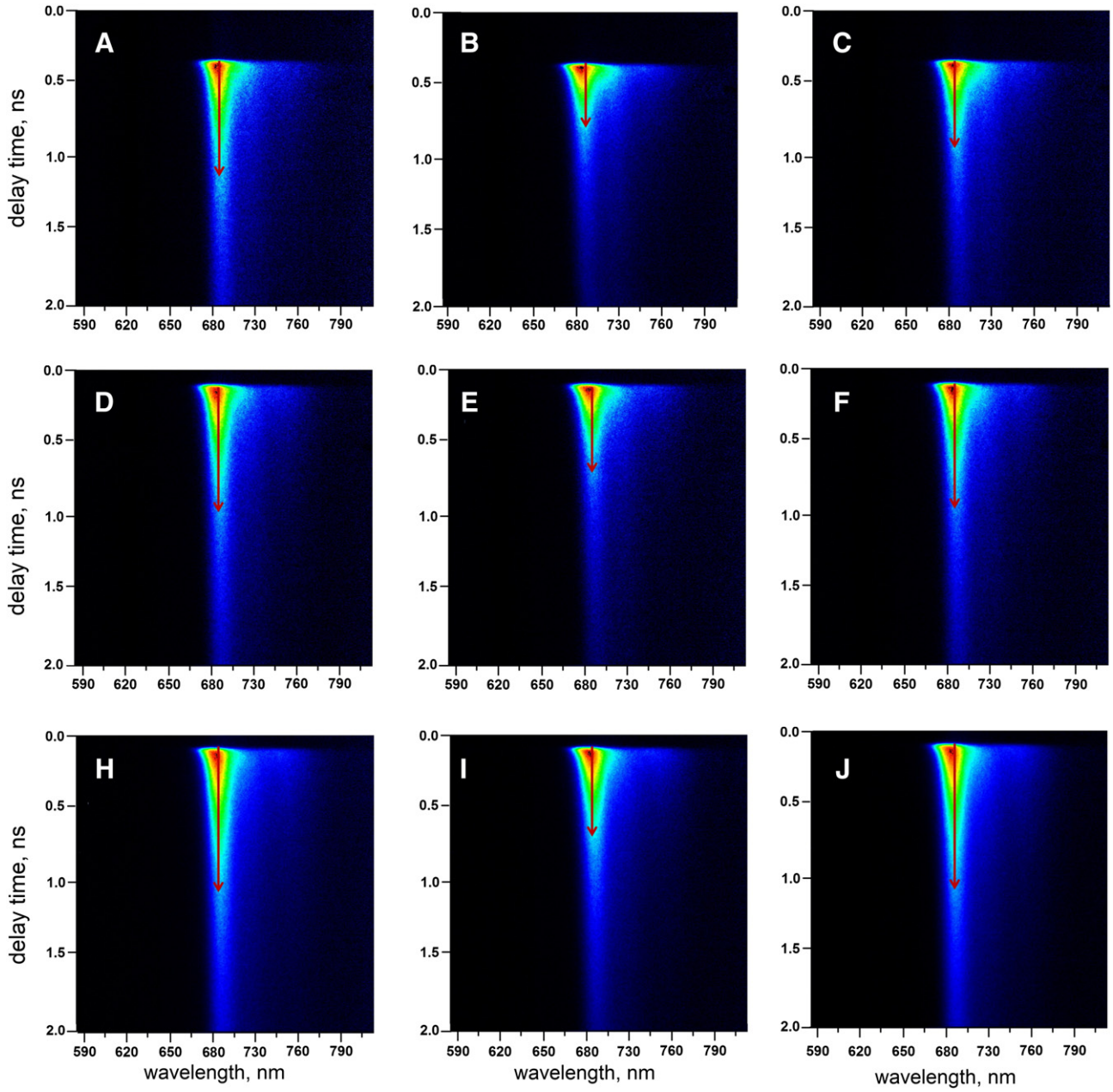

Fig. 3. Streak-camera images of unquenched (A, D, H), quenched (B, E, I) and relaxed cells (C, F, J). In panels A, B, and C Chl *a* was preferentially excited at 400 nm, in panels D, E, and F fx_{blue} and fx_{red} were excited at 490 nm while in panels H, I, and J results for $\lambda_{ex} = 550$ nm (fx_{red}) are presented. The lengths of the arrows correspond to the average lifetime detected at 685 nm.

shape of that of PSII, peaking at 685 nm with a vibronic band around 750 nm. Similar 77 K spectra were reported before for PSII preparations from higher plants [48–50] and the diatom *Chaetoceros gracilis* [51]. However, a pronounced 695-nm fluorescence maximum from red-absorbing Chls of CP47 is missing but such a peak is only observed for PSII-RC and some BBY preparations where the antenna/RC ratio is lower than in native thylakoid membranes [52–54]. For whole thylakoid membranes this band tends to disappear and only the 685 nm PSII band is observed [55]. The absence of the 695 nm peak is also typical for crude PSII preparations of *C. gracilis*, confirming that the difference spectrum represents PSII complexes with additional antenna rather than pure PSII cores [51].

After having estimated an 'in vivo' fluorescence emission spectrum of PSII complexes, this spectrum was used to determine the influence of PSII and the antenna on qE_1 by decomposing the 3rd DAS for the unquenched and quenched datasets as described in the Supplemental materials (Supplemental Fig. S4). The results for 490 nm excitation are given in Fig. 6A (for 550 nm results, see Supplemental Fig. S5). As was already found above, the PSII contribution decreases in case of NPQ while the residual spectra obtained after PSII subtraction (we term this *antenna 1* spectrum) look very similar for the unquenched and quenched datasets with a peak at 690 nm and a broad fluorescence feature between 690 nm and 720 nm. The *antenna 1* spectrum is also given in Fig. 6C and it was obtained by averaging four spectra from the 3rd DAS in the unquenched/quenched state for 490/550 nm excitation. It resembles the fluorescence emission spectrum of aggregated FCPb at 77 K as obtained in [28] (see Fig. 6C and Supplemental Fig. S4E, F). In vivo there is apparently a fraction of aggregated FCPs that is not influenced by NPQ, at least not at 77 K. In this respect it is interesting to note that both oligomeric FCPb and FCPa trimers show strong reduction of

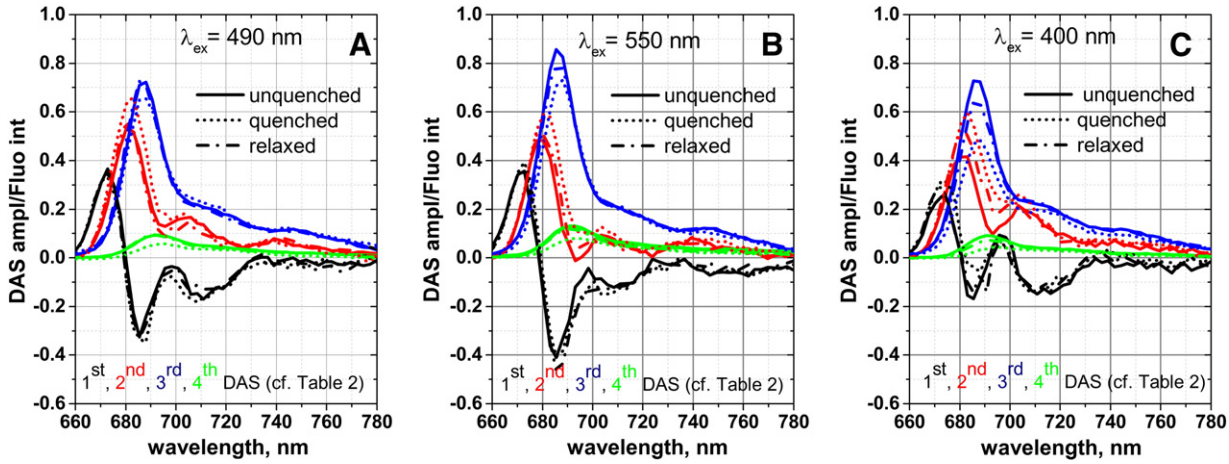

Fig. 4. DAS for unquenched (solid line), quenched (dotted line), and relaxed (dash dotted line) states obtained from global analysis of streak-camera data measured at 77 K upon 490 nm (A), 550 nm (B) and 400 nm (C) excitation. The lifetimes of the corresponding DAS are presented in Table 2 with the corresponding colors. The overall fluorescence spectra at t = 0 were normalized to each other.

fluorescence yield when being artificially aggregated by detergent removal but only FCPa trimers show ΔpH and Dtx-dependent quenching [28,29].

Thus the effect of quenching on the 3rd DAS is solely due to a reduction of PSII fluorescence, whereas FCPb is not influenced by quenching and contributes equally in both states.

3.4.2. Evidence for FCPa aggregation and quenching

The shape of the 4th component differs considerably for unquenched and quenched cells (Fig. 6B). Again the fact that PSII becomes quenched is obvious: its contribution to the area of the unquenched DAS is 20% while it is at most 8% for the quenched state. Interestingly the shape of the residual spectrum after PSII subtraction from the 4th DAS (*antenna 2*) differs substantially for the various states. For quenched cells the relative fluorescence increases in the 700–730 nm region, while the total area decreases strongly, which is a characteristic for aggregation of FCP. Also this residual spectrum is reminiscent of the 77 K fluorescence spectrum of aggregated FCPs [28]. In Fig. 6C also the residual spectra obtained from the 4th (*antenna 2*, unquenched, quenched) DAS are shown (see the legend for details). In contrast to *antenna 1* (presumably FCPb), *antenna 2* is strongly involved in qE_1, i.e. its contribution to the 4th DAS decreases substantially upon quenching. Since in vitro the ΔpH-dependent quenching is only observed for FCPa trimers but not for FCPb oligomers [28,29], and since only FCPa contains Lhcx proteins known to be involved in NPQ [14] this suggests that mostly FCPa contributes to the *antenna 2* decrease as part of qE_1. Upon 550 nm excitation, the decomposition of the longest DAS gives (somewhat) similar results (Supplemental Fig. S5). Finally, it appears that upon 490 nm excitation the decrease of the 4th DAS in the quenched state is for 35% due to the decrease of the PSII fluorescence and for 65% due to the decrease of *antenna 2* fluorescence while upon 550 nm excitation these percentages are 25% (for PSII) and 75% (for *antenna 2*).

Fig. 4 shows that the amplitude of the 2nd DAS increases upon quenching. The increase corresponds largely to a decrease in amplitude of the 3rd DAS, and to a lesser extent to that of the 4th DAS. These results are consistent with the fact that the contribution of PSII to the 3rd and 4th DAS and the contribution of *antenna 2* (presumably mostly FCPa) to the 4th DAS decrease upon quenching.

In summary, qE_1 is due to PSII complexes and aggregated FCPa complexes, while FCPb does not contribute.

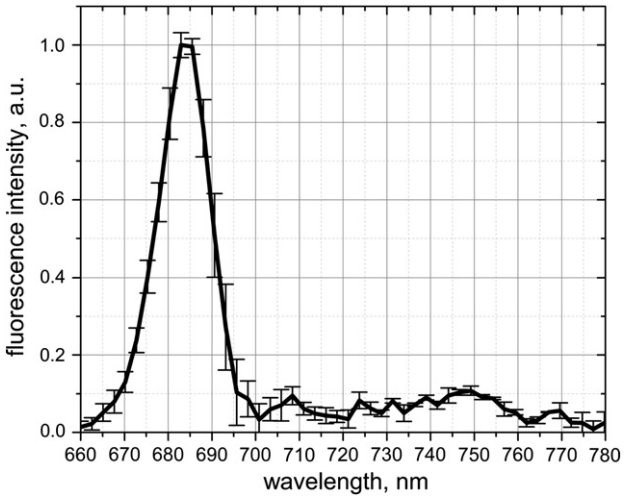

Fig. 5. Fluorescence emission spectrum of PSII complexes obtained by subtracting the 3rd (blue) DAS of quenched cells from that of unquenched cells. The procedure was repeated for all three excitation wavelengths, after which the resulting spectra were averaged. The black line represents the average spectrum and error bars reflect standard deviations.

3.5. Describing qE_2 using spectral reconstruction

3.5.1. qE_2 observed for Chl a excitation

qE_1 is observed for all excitation wavelengths while qE_2 is detected for Chl *a* excitation (400 nm) and hardly observable for fx (antenna) excitation, suggesting that qE_2 occurs in PSII cores that are not connected to the outer antenna. To confirm this, the 400 nm DAS of quenched, unquenched and relaxed cells were decomposed and the results of the 3rd component decomposition are presented in Supplemental Fig. S6A. They confirm that the difference between the quenched and relaxed states is mostly due to the contribution of PSII and not of the outer antenna. The PSII spectrum does not recover to its original unquenched state in darkness, but stays partly quenched after strong light illumination. The contribution of aggregated antenna to the 3rd DAS (*antenna 1*) remains more or less the same in all three states and it does not participate in any of the two quenching processes.

The decomposition of the 4th component is in agreement with the observations described before (Supplemental Fig. S6B). The amplitude of the residual (*antenna 2*) spectrum decreases strongly upon quenching as compared with the unquenched state, but largely recovers in darkness, reflecting again FCPa quenching as part of qE_1 but not of qE_2. The PSII contribution accounts for around 25% of the total area in the case of unquenched cells, while for the quenched state its contribution is

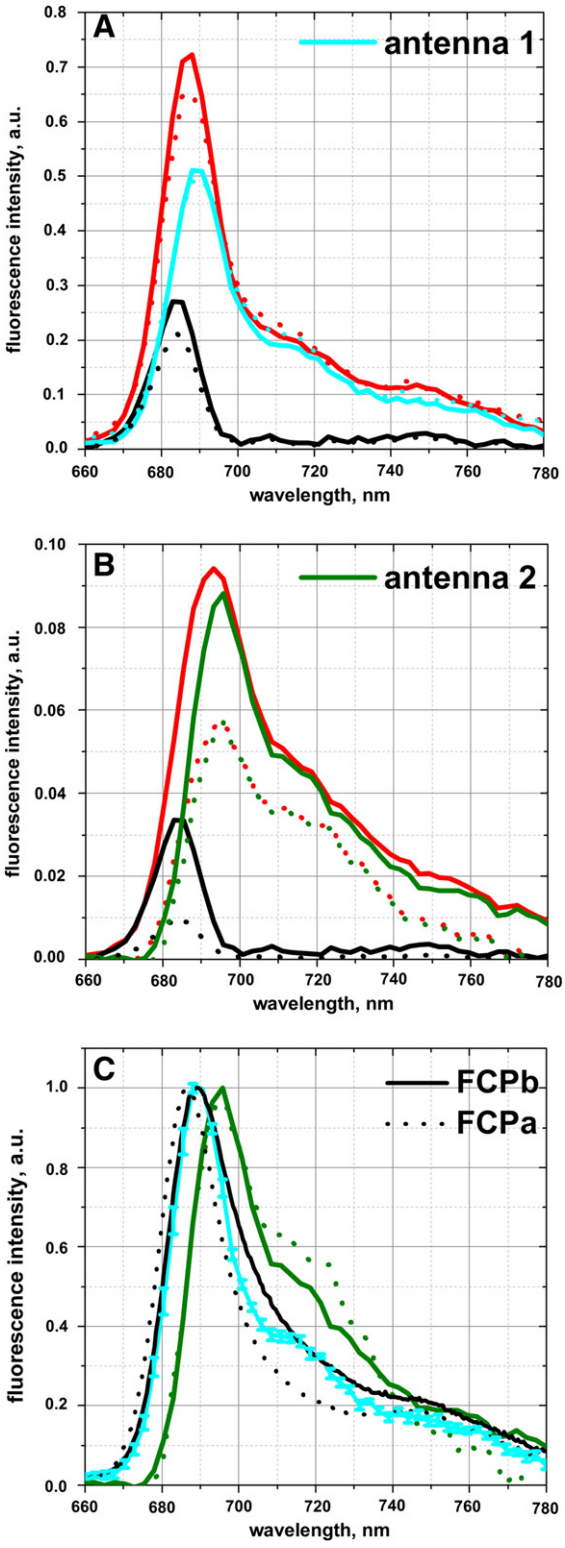

Fig. 6. Decomposition of the 3rd (A) and 4th (B) components (red lines) obtained from global analysis of unquenched (solid) and quenched (dotted) datasets upon 490 nm excitation using PSII fluorescence emission spectrum (black lines). The residual spectra in cyan and green represent different subpopulations of aggregated antenna (called *antenna 1* and *antenna 2* from the 3rd and 4th DAS, respectively). In panel C averaged and normalized *antenna 1* and *2* spectra (see text) are compared with aggregated forms of FCPb (black solid) and FCPa (black dotted) from [28]. The *antenna 2* spectra (unquenched and quenched) in panel C were obtained by averaging corresponding spectra from 490 nm and 550 nm data, since they are virtually identical for two excitation wavelengths. The *antenna 1* spectrum is an average of four spectra from the 3rd DAS in the unquenched/quenched state for 490/550 nm excitation. The error bars reflect standard deviations (C).

almost negligible. 'Relaxed' data show that the PSII fluorescence does not recover to its original unquenched state in the dark, confirming the PSII origin of qE_2. It can be concluded that qE_2 accounts for 35% of the total decrease of the PSII area of the 3rd and 4th DAS while qE_1 accounts for the remaining 65%. It should be realized that the latter percentage refers to PSII complexes that are connected to the outer antenna, so qE_1 in PSII reflects quenching of both cores and the connected antenna, whereas the 35% refers to largely disconnected PSII cores (qE_2), which does not relax in the dark and is correlated with the persistence of Dtx. Therefore, it might be that qE_2 protects even a larger amount of PSII cores, although the fluorescence quenching might at first sight suggest that qE_1 represents the dominant protection mechanism.

3.5.2. Minor effect of qE_2 for $\lambda_{ex} = 550$ nm

Although the spectra of relaxed cells closely resemble those of unquenched cells in the case of antenna excitation, a small difference between unquenched and relaxed data was still present when exciting at 550 nm (fx_{red}), but not at 490 nm (Fig. 4). Around 4% of the PSII area in the 3rd DAS is not recovered in the relaxed state upon selective fx_{red} excitation (Supplemental Fig. S7). This indicates that a small fraction of "PSII cores" is excited at 550 nm, either because it is energetically connected to very small amounts of FCPs binding preferentially fx_{red}, or because there is a small amount of Chl *a* absorption at 550 nm [41]. The 4th DAS in the relaxed state has a slightly lower amplitude while the fluorescence intensity in the PSII region (below 690 nm) hardly changes when compared to the unquenched state, implying the presence of quenching of *antenna 2*, previously attributed to FCPa. Because this is also part of the qE_2 type quenching, it is again Dtx-dependent. This quenching does not contribute more than 10% to the total quenching of the FCPa pool. This is in agreement with PAM measurements, where ~5% of the F_t amplitude (exclusively attributed to antenna NPQ [56]) remains quenched in the qE_2 state.

In summary, the qE_2 process appears to act on PSII RCs that are functionally disconnected from all or most of the antenna complexes since it is hardly observed upon fx excitation. Considering that qE_2 is observed in the relaxed state where Dtx is still present, we suggest that Dtx is responsible for this quenching and it might even be responsible for antenna detachment that leads to photoprotection of RCs (less excitations are captured) like in plants [57–59]. Although our fx_{red} excitation data indicate that those 'PSII cores' might still bind at least one antenna complex that works as a quencher, direct Dtx-related quenching of PSII cores cannot be excluded, since the presence of lipid-dissolved Dtx-cycle pigments that are not bound to FCPs has been reported [42]. Furthermore, there are some indications of direct PSII core quenching in *Phaeodactylum tricornutum*, although it was excluded that Dtx was causing that quenching [60]. From our fx_{red} excitation measurements, we also conclude that some antenna (presumably FCPa) quenching might occur during the qE_2 process, which should correspond to not more than 10% of the total fraction of FCPa.

4. Conclusions

Non-photochemical quenching in the diatom *C. meneghiniana* shows two distinct contributions: qE_1 and qE_2 (Figs. 1, 7). qE_1 is rapidly induced in strong light and also rapidly disappears again in darkness and supposedly it is directly coupled to the pH gradient across the thylakoid membrane. qE_2 is induced directly after pH gradient formation. This quenching remains present in subsequent darkness and only disappears again in the presence of a low amount of light. Its presence is directly related to the conversion of Ddx to Dtx [20]. The amount of Dtx increases in the presence of strong light but remains present after switching to darkness. qE_1 takes place in PSII with a substantial amount of antenna connected (qE_{1a}, Fig. 7) whereas also aggregated FCPa antenna complexes appear to be quenched (qE_{1b}). qE_2 takes place in PSII cores that are detached from almost all the FCP antenna although it

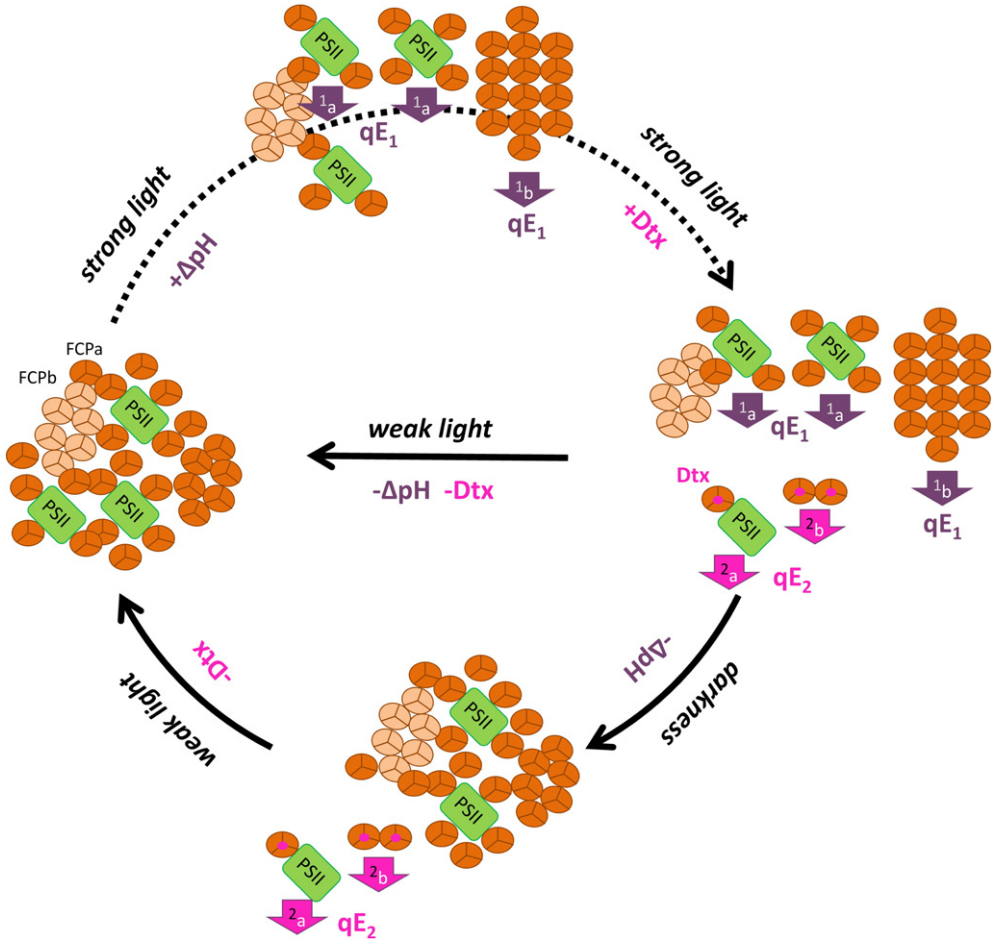

Fig. 7. Model for non-photochemical quenching in *C. meneghiniana*. In strong light two quenching mechanisms independent of diatoxanthin (Dtx) are present. The first (upper part of the fig.) represents quenching (qE_1) of the whole PSII complex (1_a) and the second is quenching of FCPa antenna that is aggregated due to ΔpH formation (1_b). With the rapid accumulation of a Dtx pool (middle right), Dtx-related quenching appears (qE_2). It is manifested by quenching of PSII that almost lack FCPs (2_a). Most probably the quenching site is located at an FCPa antenna attached to the core, although direct quenching of PSII cores cannot be excluded. This effect is accompanied with Dtx-dependent quenching of FCPa that has been disconnected from PSII complexes: 2_b (not more than 10% of the total FCPa pool). All qE_2 quenching is persistent in the darkness (lower part of the fig.), but not under weak light.

cannot be completely ruled out that there is still a very small amount of FCP bound to these cores (qE_{2a}), accompanied by very minor further quenching of aggregated FCPa complexes due to Dt (qE_{2b}). FCPb antenna complexes on the other hand remain unquenched during both qE_1 and qE_2. Therefore, it seems that upon the induction of NPQ at first FCPa aggregates in PSII become quenched, after which they partly detach from PSII cores while the quenching persists. Then the continued formation of Dtx leads to the additional quenching of isolated PSII cores and to a minor extent of aggregated FCPa complexes. Although the amount of quenching during qE_2 is smaller than during qE_1 it might be more effective because it corresponds to selective quenching of the PSII cores. In subsequent darkness the quenching of FCPa disappears while qE_2 remains present and only in the presence of some light does recovery to the fully unquenched state occur.

Acknowledgements

This work was supported by the HARVEST Marie Curie Research Training Network [PITN-GA-2009-238017 to VUC, CB and HvA]. This project was also carried out within the research program of BioSolar Cells, co-financed by the Dutch Ministry of Economic Affairs (to VUC and HvA). We thank R.B.M. Koehorst (Wageningen UR), A. van Hoek (Wageningen UR), and Dr. A. Bader (Wageningen UR) for technical help with the measurements, C. Wolfs (Wageningen UR) for initial help with growing cells, and Dr. S. Laptenok (University of East Anglia) and J. Snellenburg (VU Amsterdam University) for help with the usage of the Glotaran software analysis toolkit. Dr. R. Croce and D. de Kort are acknowledged for critical reading of the manuscript and for many helpful suggestions.

Appendix A. Supplementary data

Supplementary data to this article can be found online at http://dx.doi.org/10.1016/j.bbabio.2014.02.021.

References

[1] P.G. Falkowski, R.T. Barber, V. Smetacek, Biogeochemical controls and feedbacks on ocean primary production, Science 281 (1998) 200–206.
[2] C.B. Field, M.J. Behrenfeld, J.T. Randerson, P. Falkowski, Primary production of the biosphere: integrating terrestrial and oceanic components, Science 281 (1998) 237–240.
[3] F. Lavaud, Fast regulation of photosynthesis in diatoms: mechanisms, evolution and ecophysiology, Funct. Plant Sci. Biotechnol. 1 (2007) 267–287.
[4] D.G. Durnford, R. Aebersold, B.R. Green, The fucoxanthin–chlorophyll proteins from a chromophyte alga are part of a large multigene family: structural and evolutionary relationships to other light harvesting antennae, Mol. Gen. Genet. 253 (1996) 377–386.
[5] M. Szabo, L. Premvardhan, B. Lepetit, R. Goss, C. Wilhelm, G. Garab, Functional heterogeneity of the fucoxanthins and fucoxanthin–chlorophyll proteins in diatom cells revealed by their electrochromic response and fluorescence and linear dichroism spectra, Chem. Phys. 373 (2010) 110–114.
[6] V.U. Chukhutsina, C. Buchel, H. van Amerongen, Variations in the first steps of photosynthesis for the diatom *Cyclotella meneghiniana* grown under different light conditions, Biochim. Biophys. Acta 1827 (2013) 10–18.

[7] E. Papagiannakis, I.H.M. van Stokkum, H. Fey, C. Buchel, R. van Grondelle, Spectroscopic characterization of the excitation energy transfer in the fucoxanthin–chlorophyll protein of diatoms, Photosynth. Res. 86 (2005) 241–250.
[8] N. Gildenhoff, S. Amarie, K. Gundermann, A. Beer, C. Buchel, J. Wachtveitl, Oligomerization and pigmentation dependent excitation energy transfer in fucoxanthin–chlorophyll proteins, Biochim. Biophys. Acta 1797 (2010) 543–549.
[9] Z.F. Liu, H.C. Yan, K.B. Wang, T.Y. Kuang, J.P. Zhang, L.L. Gui, X.M. An, W.R. Chang, Crystal structure of spinach major light-harvesting complex at 2.72 Angstrom resolution, Nature 428 (2004) 287–292.
[10] C. Buchel, Fucoxanthin–chlorophyll proteins in diatoms: 18 and 19 kDa subunits assemble into different oligomeric states, Biochemistry 42 (2003) 13027–13034.
[11] A. Beer, K. Gundermann, J. Beckmann, C. Buchel, Subunit composition and pigmentation of fucoxanthin–chlorophyll proteins in diatoms: evidence for a subunit involved in diadinoxanthin and diatoxanthin binding, Biochemistry 45 (2006) 13046–13053.
[12] N. Gildenhoff, S. Amarie, A. Beer, K. Gundermann, C. Buchel, J. Wachtveitl, Light harvesting, energy transfer and photoprotection in the fucoxanthin–chlorophyll proteins of *Cyclotella meneghiniana*, Springer Ser. Chem. Phys. 92 (2009) 577–579.
[13] L. Premvardhan, L. Bordes, A. Beer, C. Buchel, B. Robert, Carotenoid structures and environments in trimeric and oligomeric fucoxanthin chlorophyll a/c(2) proteins from resonance Raman spectroscopy, J. Phys. Chem. B 113 (2009) 12565–12574.
[14] B. Bailleul, A. Rogato, A. de Martino, S. Coesel, P. Cardol, C. Bowler, A. Falciatore, G. Finazzi, An atypical member of the light-harvesting complex stress-related protein family modulates diatom responses to light, Proc. Natl. Acad. Sci. U. S. A. 107 (2010) 18214–18219.
[15] K.K. Niyogi, Photoprotection revisited: genetic and molecular approaches, Annu. Rev. Plant Physiol. Plant Mol. Biol. 50 (1999) 333–359.
[16] T.G. Owens, Light-harvesting function in the diatom *Phaeodactylum tricornutum*. 2. Distribution of excitation-energy between the photosystems, Plant Physiol. 80 (1986) 739–746.
[17] C.S. Ting, T.G. Owens, The effects of excess irradiance on photosynthesis in the marine diatom *Phaeodactylum tricornutum*, Plant Physiol. 106 (1994) 763–770.
[18] R. Goss, T. Jakob, Regulation and function of xanthophyll cycle-dependent photoprotection in algae, Photosynth. Res. 106 (2010) 103–122.
[19] A.V. Ruban, J. Lavaud, B. Rousseau, G. Guglielmi, P. Horton, A.-L. Etienne, The super-excess energy dissipation in diatom algae: comparative analysis with higher plants, Photosynth. Res. 82 (2004) 165–175.
[20] I. Grouneva, T. Jakob, C. Wilhelm, R. Goss, A new multicomponent NPQ mechanism in the diatom *Cyclotella meneghiniana*, Plant Cell Physiol. 49 (2008) 1217–1225.
[21] R. Goss, E. Ann Pinto, C. Wilhelm, M. Richter, The importance of a highly active and delta pH-regulated diatoxanthin epoxidase for the regulation of the PS II antenna function in diadinoxanthin cycle containing algae, J. Plant Physiol. 163 (2006) 1008–1021.
[22] B. van Oort, A. van Hoek, A.V. Ruban, H. van Amerongen, Aggregation of Light-Harvesting Complex II leads to formation of efficient excitation energy traps in monomeric and trimeric complexes, FEBS Lett. 581 (2007) 3528–3532.
[23] M. Wentworth, A.V. Ruban, P. Horton, Kinetic analysis of nonphotochemical quenching of chlorophyll fluorescence. 2. Isolated light-harvesting complexes, Biochemistry 40 (2001) 9902–9908.
[24] P. Horton, A.V. Ruban, Molecular design of the photosystem II light-harvesting antenna: photosynthesis and photoprotection, J. Exp. Bot. 56 (2005) 365–373.
[25] A.V. Ruban, R. Berera, C. Ilioaia, I.H.M. van Stokkum, J.T.M. Kennis, A.A. Pascal, H. van Amerongen, B. Robert, P. Horton, R. van Grondelle, Identification of a mechanism of photoprotective energy dissipation in higher plants, Nature 450 (2007) 575–578.
[26] M. Ballottari, J. Girardon, N. Betterle, T. Morosinotto, R. Bassi, Identification of the chromophores involved in aggregation-dependent energy quenching of the monomeric photosystem II antenna protein Lhcb5, J. Biol. Chem. 285 (2010) 28309–28321.
[27] Y. Miloslavina, I. Grouneva, P.H. Lambrev, B. Lepetit, R. Goss, C. Wilhelm, A.R. Holzwarth, Ultrafast fluorescence study on the location and mechanism of non-photochemical quenching in diatoms, Biochim. Biophys. Acta 1787 (2009) 1189–1197.
[28] K. Gundermann, C. Buchel, Factors determining the fluorescence yield of fucoxanthin–chlorophyll complexes (FCP) involved in non-photochemical quenching in diatoms, Biochim. Biophys. Acta Bioenerg. 1817 (2012) 1044–1052.
[29] K. Gundermann, C. Buchel, The fluorescence yield of the trimeric fucoxanthin–chlorophyll-protein FCPa in the diatom *Cyclotella meneghiniana* is dependent on the amount of bound diatoxanthin, Photosynth. Res. 95 (2008) 229–235.
[30] L. Provasoli, J.J.A. Mclaughlin, M.R. Droop, The development of artificial media for marine algae, Arch. Mikrobiol. 25 (1957) 392–428.
[31] S.t. Jeffrey, G. Humphrey, New spectrophotometric equations for determining chlorophylls a, b, c1 and c2 in higher plants, algae and natural phytoplankton, Biochem. Physiol. Pflanz. 167 (1975) 1–194.
[32] B. van Oort, A. Amunts, J.W. Borst, A. van Hoek, N. Nelson, H. van Amerongen, R. Croce, Picosecond fluorescence of intact and dissolved PSI-LHCI crystals, Biophys. J. 95 (2008) 5851–5861.
[33] B. Van Oort, S. Murali, E. Wientjes, R.B.M. Koehorst, R.B. Spruijt, A. van Hoek, R. Croce, H. van Amerongen, Ultrafast resonance energy transfer from a site-specifically attached fluorescent chromophore reveals the folding of the N-terminal domain of CP29, Chem. Phys. 357 (2009) 113–119.
[34] I.H.M. van Stokkum, B. van Oort, F. van Mourik, B. Gobets, H. van Amerongen, (Sub)-picosecond spectral evolution of fluorescence studied with a synchroscan streak-camera system and target analysis, Biophysical Techniques in Photosynthesis, Springer, Dordrecht, 2008, pp. 223–240.
[35] K. Broess, G. Trinkunas, C.D. van der Weij-de Wit, J.P. Dekker, A. van Hoek, H. van Amerongen, Excitation energy transfer and charge separation in photosystem II membranes revisited, Biophys. J. 91 (2006) 3776–3786.
[36] K.M. Mullen, I.H.M. van Stokkum, TIMP: an R package for modeling multi-way spectroscopic measurements, J. Stat. Softw. 18 (2007).
[37] I.H.M. van Stokkum, B. Gobets, T. Gensch, F. van Mourik, K.J. Hellingwerf, R. van Grondelle, J.T.M. Kennis, (Sub)-picosecond spectral evolution of fluorescence in photoactive proteins studied with a synchroscan streak camera system, Photochem. Photobiol. 82 (2006) 380–388.
[38] A. Beer, M. Juhas, C. Buchel, Influence of different light intensities and different iron nutrition on the photosynthetic apparatus in the diatom *Cyclotella meneghiniana* (Bacillariophyceae), J. Phycol. 47 (2011) 1266–1273.
[39] J. Lavaud, B. Rousseau, A.-L. Etienne, In diatoms, a transthylakoid proton gradient alone is not sufficient to induce a non-photochemical fluorescence quenching, FEBS Lett. 523 (2002) 163–166.
[40] I. Grouneva, T. Jakob, C. Wilhelm, R. Goss, The regulation of xanthophyll cycle activity and of non-photochemical fluorescence quenching by two alternative electron flows in the diatoms *Phaeodactylum tricornutum* and *Cyclotella meneghiniana*, Biochim. Biophys. Acta Bioenerg. 1787 (2009) 929–938.
[41] L. Premvardhan, D.J. Sandberg, H. Fey, R.R. Birge, C. Buchel, R. van Grondelle, The charge-transfer properties of the S-2 state of fucoxanthin in solution and in fucoxanthin chlorophyll-a/c(2) protein (FCP) based on stark spectroscopy and molecular-orbital theory, J. Phys. Chem. B 112 (2008) 11838–11853.
[42] B. Lepetit, D. Volke, M. Gilbert, C. Wilhelm, R. Goss, Evidence for the existence of one antenna-associated, lipid-dissolved and two protein-bound pools of diadinoxanthin cycle pigments in diatoms, Plant Physiol. 154 (2010) 1905–1920.
[43] T. Veith, C. Buchel, The monomeric photosystem I-complex of the diatom *Phaeodactylum tricornutum* binds specific fucoxanthin chlorophyll proteins (FCPs) as light-harvesting complexes, Biochim. Biophys. Acta Bioenerg. 1767 (2007) 1428–1435.
[44] A. Yamagishi, Y. Ikeda, M. Komura, H. Koike, K. Satoh, S. Itoh, Y. Shibata, Shallow sink in an antenna pigment system of photosystem I of a marine centric diatom, *Chaetoceros gracilis*, revealed by ultrafast fluorescence spectroscopy at 17 K, J. Phys. Chem. B 114 (2010) 9031–9038.
[45] Y. Ikeda, M. Komura, M. Watanabe, C. Minami, H. Koike, S. Itoh, Y. Kashino, K. Satoh, Photosystem I complexes associated with fucoxanthin–chlorophyll-binding proteins from a marine centric diatom, *Chaetoceros gracilis*, Biochim. Biophys. Acta 1777 (2008) 351–361.
[46] C.D. van der Weij-de Wit, J.A. Ihalainen, R. van Grondelle, J.P. Dekker, Excitation energy transfer in native and unstacked thylakoid membranes studied by low temperature and ultrafast fluorescence spectroscopy, Photosynth. Res. 93 (2007) 173–182.
[47] M. Tikkanen, M. Nurmi, M. Suorsa, R. Danielsson, F. Mamedov, S. Styring, E.M. Aro, Phosphorylation-dependent regulation of excitation energy distribution between the two photosystems in higher plants, Biochim. Biophys. Acta 1777 (2008) 425–432.
[48] E.G. Andrizhiyevskaya, A. Chojnicka, J.A. Bautista, B.A. Diner, R. van Grondelle, J.P. Dekker, Origin of the F685 and F695 fluorescence in Photosystem II, Photosynth. Res. 84 (2005) 173–180.
[49] R. Van Dorssen, J. Plijter, J.P. Dekker, A. Den Ouden, J. Amesz, H. Van Gorkom, Spectroscopic properties of chloroplast grana membranes and of the core of photosystem II, Biochim. Biophys. Acta Bioenerg. 890 (1987) 134–143.
[50] R. Van Dorssen, J. Breton, J. Plijter, K. Satoh, H. Van Gorkom, J. Amesz, Spectroscopic properties of the reaction center and of the 47 kDa chlorophyll protein of photosystem II, Biochim. Biophys. Acta Bioenerg. 893 (1987) 267–274.
[51] R. Nagao, T. Tomo, E. Noguchi, S. Nakajima, T. Suzuki, A. Okumura, Y. Kashino, M. Mimuro, M. Ikeuchi, I. Enami, Purification and characterization of a stable oxygen-evolving Photosystem II complex from a marine centric diatom, *Chaetoceros gracilis*, Biochim. Biophys. Acta Bioenerg. 1797 (2010) 160–166.
[52] R. Croce, H. van Amerongen, Light-harvesting and structural organization of Photosystem II: from individual complexes to thylakoid membrane, J. Photochem. Photobiol. B 104 (2011) 142–153.
[53] K. Broess, G. Trinkunas, A. van Hoek, R. Croce, H. van Amerongen, Determination of the excitation migration time in Photosystem II consequences for the membrane organization and charge separation parameters, Biochim. Biophys. Acta 1777 (2008) 404–409.
[54] B. van Oort, M. Alberts, S. de Bianchi, L. Dall'Osto, R. Bassi, G. Trinkunas, R. Croce, H. van Amerongen, Effect of antenna-depletion in Photosystem II on excitation energy transfer in *Arabidopsis thaliana*, Biophys. J. 98 (2010) 922–931.
[55] J. Bennett, K.E. Steinback, C.J. Arntzen, Chloroplast phosphoproteins: regulation of excitation energy transfer by phosphorylation of thylakoid membrane polypeptides, Proc. Natl. Acad. Sci. U. S. A. 77 (1980) 5253–5257.
[56] B. Demmig-Adams, W.W. Adams, U. Heber, S. Neimanis, K. Winter, A. Kruger, F.C. Czygan, W. Bilger, O. Bjorkman, Inhibition of zeaxanthin formation and of rapid changes in radiationless energy dissipation by dithiothreitol in spinach leaves and chloroplasts, Plant Physiol. 92 (1990) 293–301.
[57] Y. Miloslavina, A. Wehner, P.H. Lambrev, E. Wientjes, M. Reus, G. Garab, R. Croce, A.R. Holzwarth, Far-red fluorescence: a direct spectroscopic marker for LHCII oligomer formation in non-photochemical quenching, FEBS Lett. 582 (2008) 3625–3631.
[58] M.P. Johnson, T.K. Goral, C.D.P. Duffy, A.P. Brain, C.W. Mullineaux, A.V. Ruban, Photoprotective energy dissipation involves the reorganization of photosystem II light-harvesting complexes in the grana membranes of spinach chloroplasts, Plant Cell 23 (2011) 1468–1479.
[59] A.V. Ruban, M.P. Johnson, C.D.P. Duffy, The photoprotective molecular switch in the photosystem II antenna, Biochim. Biophys. Acta Bioenerg. 1817 (2012) 167–181.
[60] D. Eisenstadt, I. Ohad, N. Keren, A. Kaplan, Changes in the photosynthetic reaction centre II in the diatom *Phaeodactylum tricornutum* result in non-photochemical fluorescence quenching, Environ. Microbiol. 10 (2008) 1997–2007.